Applied Surface Science 273 (2013) 607–612

Applied Surface Science

journal homepage: www.elsevier.com/locate/apsusc

Sensitivity of photoelectron energy loss spectroscopy to surface reconstruction of microcrystalline diamond films

Denis G.F. David [a], Marie-Amandine Pinault-Thaury [b], Dominique Ballutaud [b], Christian Godet [c,*]

[a] Instituto de Física, Universidade Federal da Bahia, Campus Universitário de Ondina, 40.210-340 Salvador, Bahia, Brazil
[b] GEMaC, UMR 8635 – CNRS, 1 place Aristide Briand, 92195 Meudon Cedex, France
[c] Physique des Surfaces et Interfaces, Institut de Physique de Rennes (CNRS UMR 6251), Université Rennes 1, Beaulieu – Bât. 11E – 35042 Rennes, France

ARTICLE INFO

Article history:
Received 12 November 2012
Received in revised form 1 February 2013
Accepted 19 February 2013
Available online 27 February 2013

Keywords:
XPS
Electron energy loss
Plasmon
Diamond
Surface reconstruction

ABSTRACT

In X-ray Photoelectron Spectroscopy (XPS), binding energies and intensities of core level peaks are commonly used for chemical analysis of solid surfaces, after subtraction of a background signal. This background due to photoelectron energy losses to electronic excitations in the solid (surface and bulk plasmon excitation, inter band transitions) contains valuable information related to the near surface dielectric function $\varepsilon(\hbar\omega)$. In this work, the sensitivity of Photoelectron Energy Loss Spectroscopy (PEELS) is investigated using a model system, namely the well-controlled surface reconstruction of diamond. Boron-doped microcrystalline thin films with a mixture of (1 1 1) and (1 0 0) preferential orientations were characterized in the as-grown state, with a partially hydrogenated surface, and after annealing at 1150 °C in ultra high vacuum. After annealing, the bulk $(\sigma+\pi)$ plasmon of diamond at 34.5 eV is weakly attenuated but no evidence for surface graphitization is observed near 6 eV, as confirmed by electronic properties. Unexpected features which appear at 10 ± 1 eV and 19 ± 1 eV in the energy loss distribution are well described by simulation of surface plasmon excitations in graphite-like materials; alternatively, they also coincide with experimental inter band transition losses in some graphene layers. This comparative study shows that the PEELS technique gives a clear signature of weak effects in the diamond surface reconstruction, even in the absence of graphitization. It confirms the sensitivity of PEELS acquisition with standard XPS equipment as a complementary tool for surface analysis.

1. Introduction

In X-ray Photoelectron Spectroscopy (XPS) studies, kinetic energies and intensities of core level photoelectrons emitted from the different atoms located in the subsurface region are commonly used for chemical analysis of solid surfaces, after subtraction of a background signal arising from energy losses to electronic excitations in the solid [1–4]. During their transport and escape through the solid surface, photoelectrons experience elastic and inelastic interactions which occur both in the bulk and at the surface; such extrinsic energy losses related to inter band transitions and plasmon excitations induce, respectively, a tailing of the primary core level peak over several eV and a broad energy distribution over several tens of eV, on the low kinetic energy side [1–6]. Hence the energy loss distribution in Photoelectron Energy Loss Spectroscopy (PEELS) contains valuable information related to the near surface dielectric function $\varepsilon(\hbar\omega)$.

It is emphasized that XPS and PEELS acquisitions are performed in the same run and at the same location of the sample (although with possibly different energy resolution and signal-to-noise ratio) in contrast with studies combining XPS and reflection EELS (REELS). In addition, angular PEELS analysis can be readily performed using conventional laboratory XPS spectrometers, while for specific studies, synchrotron light sources provide better spatial and spectral resolutions. The physics and surface sensitivity of plasmon losses in PEELS and REELS are similar in principle, except for the presence of the electron–hole interaction and the lack of a collimated beam in photoelectron spectroscopy. However, the REELS technique uses a primary electron beam generated by a field emission gun which may damage fragile samples.

This work aims at assessing the sensitivity of PEELS using a model system, namely the well-controlled surface reconstruction of diamond films upon annealing in ultra high vacuum. Diamond is a wide band gap semiconductor which has been extensively studied for its outstanding robustness and surface electronic properties. A true negative electron affinity is found for the hydrogenated surface

* Corresponding author at: EPSI – IPR (Bât. 11E – Beaulieu), Université Rennes 1, 35042 RENNES, France. Tel.: +33 2 23 23 57 06; fax: +33 2 23 23 61 98.
E-mail address: christian.godet@univ-rennes1.fr (C. Godet).

0169-4332/$ – see front matter © 2013 Elsevier B.V. All rights reserved.
http://dx.doi.org/10.1016/j.apsusc.2013.02.087

[7] making diamond an efficient photo emitter while a fairly high p-type surface conductivity is observed after air exposure [8]. The negative electron affinity is related to surface C—H dipoles while the high surface density of holes is explained by electron transfer from the diamond valence band to the deeper chemical potential in the adsorbed water layer containing protons, screened by water molecules and their corresponding carbonate anions [8,9].

Photoelectron spectroscopy studies have been performed in order to characterize the electron affinity and work function of hydrogen-terminated diamond surfaces, for both (1 1 1) and (1 0 0) orientations [10]. XPS and UPS were used to study the partial hydrogen coverage and the variety of oxygen containing chemical functionalities in the as-grown state, after intentional surface hydrogenation and after liquid phase or gas phase oxidation [11–14]. Alternatively, High Resolution EELS has been used to follow changes in surface chemical bonds after hydrogenation or annealing steps [15].

Energy loss spectroscopy of photoelectrons emitted from the C1s core level has been used previously either for investigations of the role of surface hydrogen and oxygen atom coverage [11,12] as well as for the study of seeding and growth of nano- and microcrystalline diamond films [16–19]. For the assessment of the non diamond residual phase, the ratio of the bulk ($\sigma+\pi$) plasmon loss of the diamond phase to the main C1s line (characteristic of the near-surface over typically 5 nm) was tentatively correlated to the ratio of G and D lines in Raman spectra (characteristic of a bulk depth >100 nm) [17].

Surface reconstruction of diamond films has been widely studied, both experimentally [20,21] and theoretically [22,23]. Some atomistic models have been proposed to take into account the incomplete removal of oxygen atoms along with the sp^3 to sp^2 carbon atom conversion. On both (1 0 0) and (1 1 1) surfaces, which are the dominant orientations in our microcrystalline diamond films, removal of terminating H atoms leads to a 2×1 reconstruction (dimerisation of two dangling bonds on C atoms, forming a C=C bond) [23].

Previous studies show that a higher annealing temperature is required for microcrystalline diamond reconstruction [14] as compared with nanodiamond films [15,24]. In this work, annealing conditions at 1150 °C in Ultra High Vacuum (UHV) were chosen to obtain complete desorption of hydrogen at the diamond surface which leads to some surface reconstruction of carbon atom bonding, as shown previously [14]; in the absence of extensive graphitization, such weak surface changes are not detectable in bulk Raman spectra and make this reconstruction process suitable for assessing the sensitivity of PEELS analysis. Interpretation of the plasmon loss features experimentally observed in PEELS difference spectra is tentatively performed by comparison with surface and bulk plasmon loss functions calculated using the tabulated dielectric functions of single crystal diamond [25] and graphite [26].

2. Experimental

2.1. Diamond films synthesis and characterization

Microcrystalline boron doped diamond films ($[B]=10^{19}\,cm^{-3}$) were deposited on silicon substrates by hot filament chemical vapor decomposition of hydrocarbons. The samples were kept in air. The as-grown samples were submitted to anneal under UHV at 1150 °C during 6 h. While a one hour annealing at 850 °C (under 10^{-9} Torr) is sufficient to remove most of hydrogen atoms covalently bonded to the surface [7], annealing at 1150 °C leads to complete effusion of both surface and bulk hydrogen.

The diamond structure of the samples was characterized by Ultraviolet (UV) Raman spectroscopy (laser excitation: 325 nm) before and after annealing. The XPS measurements were carried out in a VG 220i XL system, with a base pressure of 5×10^{-10} Torr, using a monochromatized Al Kα (1486.5 eV) X-ray source with a pass energy of 20 eV (analyzer resolution 0.2 eV). Energy levels were calibrated with a Au single crystal. The spectra were processed using the VG Eclipse Datasystem software, using Voigt profiles and a Shirley background contribution [1] which is included in the fitting process.

2.2. PEELS analysis

In carbon based materials, the C1s core level peak at a binding energy $E_B\approx285$ eV is followed by a structured background extending toward higher binding (lower kinetic) energies. This broad loss spectrum corresponds to C1s photoelectrons that have suffered energy losses on their way to the sample surface (and across the sample surface) and it is thus characteristic for the sample under investigation. Plasmon losses are a direct consequence of the dielectric response of the film to the external electromagnetic radiation. Collective excitations (plasmons) run as longitudinal charge density oscillations through the volume of the solid and along its surface.

The sensitivity of surface and bulk plasmon excitation to surface reconstruction of diamond thin films is investigated by PEELS, over the energy range 0–90 eV. The zero of the energy loss scale is taken at the energy of the C1s peak (zero-loss peak) maximum and the spectra are normalized to a common height of this so-called zero-loss peak. Fermi level changes are thus compensated by the PEELS analysis procedure. A constant background subtraction is performed for setting to zero the high kinetic energy side of the C1s peak. Since this study is performed with a monochromatized X-ray source, subtraction of the satellite signal is not required.

Single (34.5 eV) and multiple bulk plasmon excitations of diamond dominate at large loss energies, while surface excitations and inter band transitions are expected to dominate the energy loss distribution at lower energies. Note that loss features at very low energies are difficult to observe in PEELS due to the broad C1s line resulting from a variety of chemical environments (ether, carbonyl) of C atoms. This is the case, e.g. for transitions from valence band to unoccupied surface defect levels within the band gap, previously observed by EELS near 2 eV [27].

A practical method has been proposed [28] to derive the single plasmon loss distribution Im $[-1/\varepsilon(\hbar\omega)]$ from XPS data, following the technique developed by Egerton [6] and Werner [5] for Electron Energy Loss Spectroscopy (EELS). Such analysis of PEELS experimental spectra includes deconvolution of multiple plasmon losses and separation of bulk vs surface plasmon excitations. Careful removal of single-electron scattering (e.g. inter band transitions) at low loss energy is a prerequisite step to derive the single plasmon loss distribution.

In recent work [28], several methods were compared to separate inter band transitions from bulk or surface plasmons excitation, taking amorphous silicon as a well-known reference material. In diamond films, the analysis is more complicated because inter band transitions occur at higher energies ($\hbar\omega<25$ eV) with a peak around 12 eV in the dielectric function calculated from tabulated optical index data [25]. Since it deserves more detailed developments, the dielectric function obtained from PEELS data using our inversion algorithm will be reported elsewhere [29]. Hence, this study is focused on qualitative information derived from the difference in energy loss functions, before and after annealing, in the loss energy range (smaller than 25 eV) where multiple scattering events can be neglected.

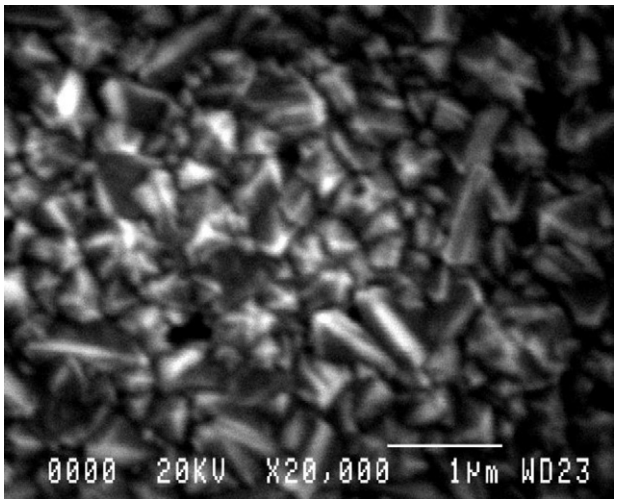

Fig. 1. Scanning electron microscopy image of the microcrystalline diamond film grown on a Si(1 0 0) substrate, with a mixture of (1 1 1) and (1 0 0) preferential orientations (pyramids and biplanes, respectively).

3. Experimental results

Hydrogenation/thermal desorption experiments have been repeated several times in order to perform electrochemical characterizations with microcrystalline diamond electrodes, with a good reproducibility of their surface chemistry and electronic properties after hydrogenation and annealing. The PEELS results presented here correspond to a typical microcrystalline diamond sample, which has been characterized in detail in a previous publication (Ref. [14]). Scanning Electron Microscopy (SEM) images of 2 μm thick microcrystalline diamond films show an average grain size of 0.5 μm with mainly (1 0 0) and (1 1 1) texture (Fig. 1). Secondary Ion Mass Spectrometry (SIMS) profiles exhibit uniform bulk hydrogen content (1×10^{20} at. cm^{-3}) which is removed after UHV anneal (1150 °C).

3.1. Raman

UV Raman spectroscopy (laser excitation: 325 nm) does not show obvious changes in the bulk diamond structure after UHV annealing at 1150 °C (Fig. 2). Comparison of the intensity of the 1332 cm^{-1} diamond line with the intensity of the broad D and G lines at 1350 and 1565 cm^{-1} shows that carbon sp^2 bond concentration in the bulk is less than 1% [30]. Such sp^2 graphitic defects may be present at microcrystalline diamond internal surfaces, due to a high density of grain boundaries and dislocations.

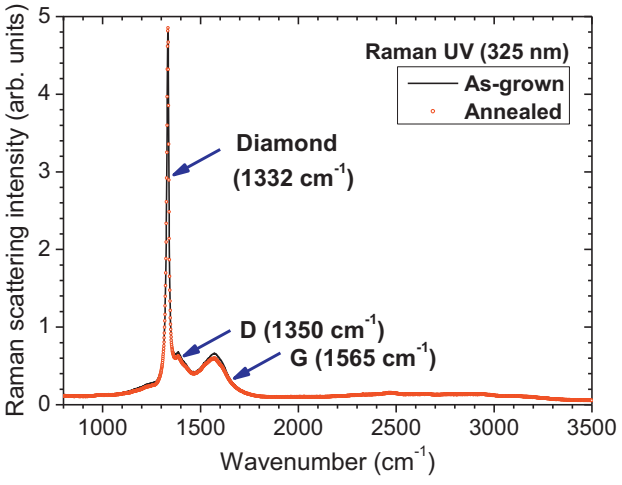

Fig. 2. UV Raman spectra of microcrystalline diamond, as-grown and after thermal annealing (1150 °C) in UHV.

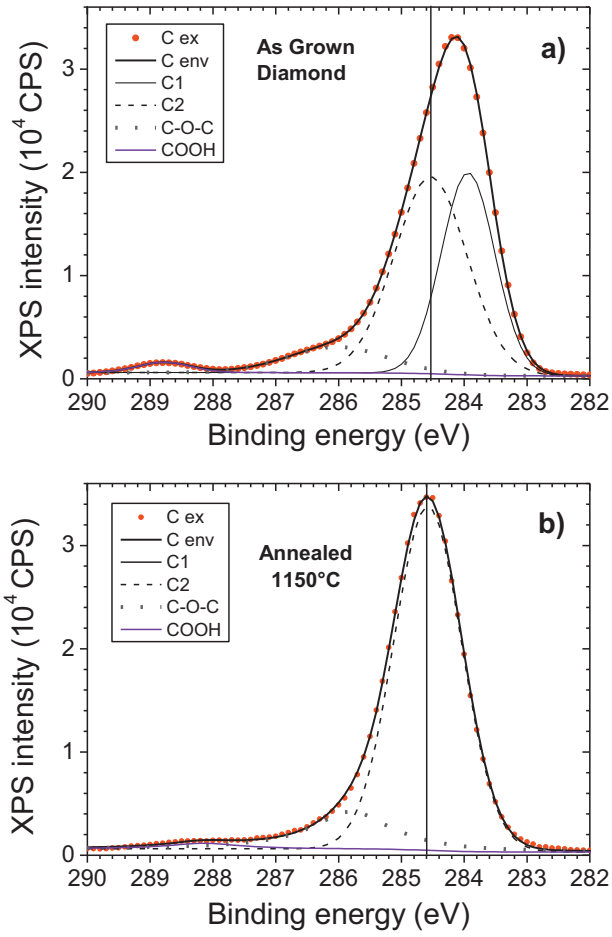

Fig. 3. Decomposition of the XPS C1s spectra of microcrystalline diamond, as-grown (a) and after thermal annealing (1150 °C) in UHV (b).

3.2. XPS

Chemical modifications and reconstruction of the diamond surface which appear after UHV annealing (Figs. 3 and 4) were discussed previously [14] in terms of carbon and oxygen bonding and band bending (hole accumulation layer) induced by adsorbed water.

The C1s XPS spectrum for the as-grown sample (kept at the ambient atmosphere) is reported in Fig. 3a. It is decomposed into four lines at respectively 283.8 eV (labeled C1), 284.5 eV (labeled C2), 286.0 and 288.7 eV. It has been suggested [14] that these different lines are the result of a partly hydrogenated surface. The components at 286.0 and 288.7 eV are attributed to C—O—C ether bonds (286.0 eV) and to COOH carboxyl functions (288.7 eV). The main peak (C2) corresponding to C—C sp^3 is found at 284.5 eV below the Fermi level (before and after UHV anneal) because strong boron doping induces a shift of the Fermi level toward the valence band.

After UHV annealing, component C1 (283.9 eV) has disappeared (Fig. 3b); this is explained by a vanishing of the hole accumulation layer (electron transfer from diamond to the physisorbed water layer) and loss of the chemisorbed surface hydrogen atoms (C—H bonds) [8,14]. Besides the main line C2 at 284.7 eV, a decrease of

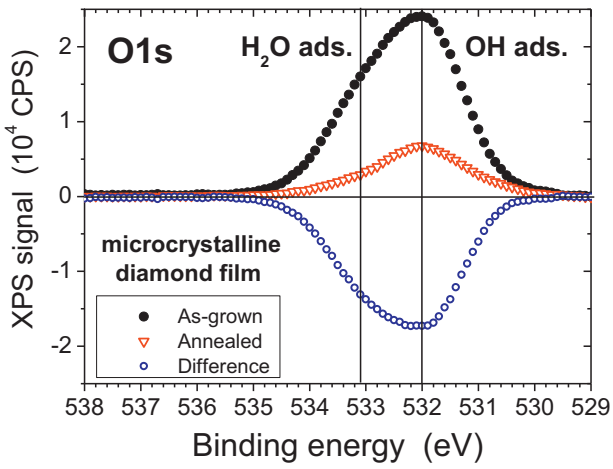

Fig. 4. XPS O1s spectra of as-grown and annealed (1150 °C) microcrystalline diamond; the difference O1s spectrum shows that both adsorbed H_2O and OH environments are partially desorbed after UHV annealing.

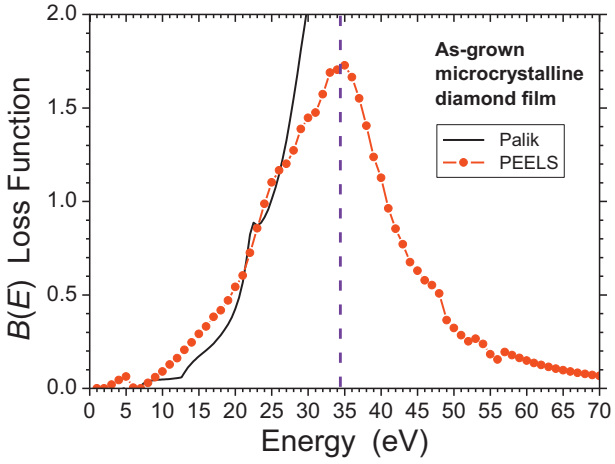

Fig. 6. Bulk loss function (full dots) derived from PEELS data for the as-grown state of microcrystalline diamond (Fig. 5) as compared with $B(E)$ derived from optical data (Palik, Ref. [25]) (full line). The peak in the single $(\sigma+\pi)$ bulk plasmon loss distribution is located at 34.5 eV.

the COOH component (288.4 eV) and an increase of the C—O—C component (285.9 eV) are observed.

The O1s XPS spectra, before and after annealing, are reported in Fig. 4. Although the O1s core level is weakly sensitive to oxygen atom binding environment, we observe at least two components, with peak positions which coincide with adsorbed H_2O/OH as measured recently on oxidized silicon surfaces [31]. The difference spectrum is consistent with the removal of both physisorbed water and either physisorbed or chemisorbed R—OH hydrocarbons (including acid and alcohol functionalities).

3.3. PEELS

The normalized PEELS spectra are reported in Fig. 5, for the diamond film measured at normal emission angle before (crosses) and after (full dots) UHV annealing. The observation of weak changes, on the order of 1% of the main C1s peak intensity, illustrates the requirement of a very good signal-to-noise ratio for PEELS analysis.

The first plasmon loss of as-grown diamond appears near 34 eV, along with contributions of multiple bulk plasmon losses up to third order over the range 0–90 eV. Using a deconvolution method given

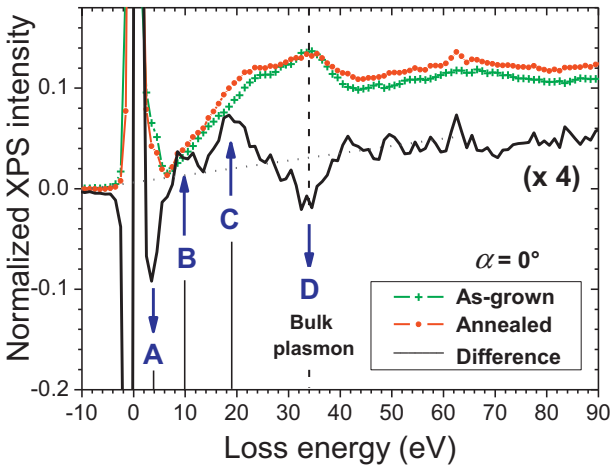

Fig. 5. Normalized energy loss distribution of C1s photoelectrons escaping the diamond surface at normal emission angle: as-grown (crosses) and after thermal annealing (circles). The difference spectrum (full line) shows attenuation of the bulk $(\sigma+\pi)$ plasmon (D) at 34 eV and enhancement of surface components at 10 ± 1 eV (peak B) and 19 ± 1 eV (peak C). Negative peak A corresponds to a decrease of O=C—OH functionalities.

in Ref. [5], the function $B(E)=\mathrm{Im}[-1/\varepsilon(\hbar\omega)]$, related to the single bulk $(\sigma+\pi)$ plasmon loss distribution, is peaked at 34.5 ± 0.5 eV (Fig. 6); a broadening of the loss distribution is observed as compared with $B(E)$ calculated from optical data [25]. In Fig. 5, the shoulder found near 21 eV is attributed to the corresponding surface plasmon; it is possibly enhanced by off-normal photoelectron emission at individual crystallite surfaces (typically 45°–55°). As emphasized before, determination of the $(\sigma+\pi)$ surface plasmon loss distribution, centered at 20.5 ± 1 eV, remains quite sensitive to the accurate removal of inter band transitions.

The difference spectrum (full line in Fig. 5) clearly shows various positive and negative contributions: (i) some carboxyl (O—C=O) moieties are eliminated at the film surface (negative peak A at 4 eV); (ii) the bulk $(\sigma+\pi)$ plasmon of diamond (negative peak D at 34 eV) is weakly attenuated; (iii) characteristic features near 10 ± 1 eV (positive peak B) and 19 ± 1 eV (positive peak C) appear in the loss distribution after annealing; (iv) in contrast, the lack of any feature at 6–7 eV, taken as a signature of graphitization in π-bonded systems, is an important result which reveals the absence of spatially extended and ordered graphitic structures [15,32,33].

These qualitative results show that the PEELS technique gives a clear signature of weak effects in the diamond surface reconstruction, even in the absence of graphitization. The possible origin of the unexpected peaks B and C is discussed in the next Section.

4. Discussion

In this work, the sensitivity of PEELS to reconstruction of microcrystalline diamond film surfaces is addressed and discussed in the broader context of carbon-based materials.

4.1. Carbon-based materials

In carbon-based materials, the energy distribution of plasmon excitations is expected to be sensitive to a variety of chemical modifications: (a) some sp^3–sp^2 conversion in the carbon atom hybridization might affect both surface and bulk (grain boundaries) $(\sigma+\pi)$ plasmon excitation due to a change in the atom density [34]; (b) spatial extension and ordering in graphitic structures may affect the intensity of the π–π^* transition feature near 6 eV [27]; (c) the surface $(\sigma+\pi)$ plasmon excitation probability (SEP) is dependent on the allotropic form of carbon [35] and it could also be sensitive to changes in the surface termination, related either to C—H and C=O

dipole coverage or to variations in the hole accumulation layer at the diamond surface.

Such effects have indeed been observed in previous PEELS studies of amorphous carbon (a-C) films: (i) several works have shown that the plasmon energy increases monotonously as a function of the average sp^3 hybridization [36–38], (ii) UHV annealing of a-C above 600 °C produces a π–π^* transition feature at 5.5 eV without affecting the bulk plasmon loss distribution (Fig. 3 in Ref. [39]), (iii) angular PEELS analysis of sp^3-rich amorphous carbon films, grown by pulsed laser deposition, has given evidence of a significant increase of the SEP after immobilization of a dense molecular monolayer, using either perfluorinated or ester functionalized organic molecules, without affecting the bulk plasmon loss distribution [39].

In the context of carbon-based materials, modeling of the loss distribution may thus be helpful for an accurate interpretation of this broad range of energy loss effects.

4.2. Diamond surface reconstruction

We have used the diamond surface reconstruction process to estimate the sensitivity of the PEELS technique for surface analysis. This process has been widely characterized by XPS but, to our best knowledge, this is the first qualitative analysis by PEELS, which limits comparison with previous work.

In this study, XPS results indicate that the as-grown microcrystalline diamond film is partly hydrogenated. In the C1s core level (Fig. 3), the large C1 peak at 283.9 eV is attributed to an upward surface band bending (hole accumulation consistent with previous studies of air-exposed samples [8,14]). Peak C2 at 284.6 eV is due to sp^3 C atoms below this nanometer-thick region. Peak C1 disappears after annealing, consistent with the observed removal of the p^+ surface layer and the so-called "transfer doping model" proposed by Maier et al. [8] to explain the surface conductivity.

It is stressed that XPS (Fig. 3) shows no evidence for a surface sp^2 C1s component after annealing, which sets an upper limit for sp^2 C smaller than one monolayer. Independent electrical characterizations after annealing show that: (i) the p^+ surface layer is no longer observed in Hall conductivity and (ii) the wide electrochemical window typical of pure diamond is maintained [40], which would not be the case if a graphitic layer were present at the surface. Both XPS and electrical results are thus consistent with PEELS data which give no evidence of graphitization, in the sense of some formation of a "conductive surface" made of nanometer-size layer.

In order to propose an interpretation to the unexpected peaks B and C (Fig. 5), the dielectric theory was used to calculate bulk and surface plasmon distributions, respectively proportional to

$$B(\hbar\omega) = Im[-1/\varepsilon(\hbar\omega)] \tag{1a}$$

and

$$S(\hbar\omega) = Im[(\varepsilon(\hbar\omega) - 1)^2/\varepsilon(\hbar\omega)(1 + \varepsilon(\hbar\omega))]$$
$$= Im[(1/\varepsilon(\hbar\omega)) - (4/1 + \varepsilon(\hbar\omega))], \tag{1b}$$

where $\varepsilon(\hbar\omega)$ is the dielectric function. The surface and bulk loss functions (Eqs. (1a) and (1b)) were calculated using tabulated optical dielectric functions of diamond [25] and graphite (ordinary index) [26]. The results are shown in Fig. 7 where we have also marked as gray areas the positions of peaks B and C obtained experimentally (Fig. 5). Inclusion of multiple losses would not significantly affect the main calculated features in the energy range below 30 eV shown in Fig. 7.

Note that the shoulder near 21 eV observed previously in experimental energy loss distribution of diamond has been attributed either to inter band transitions [41] or to a surface plasmon mode

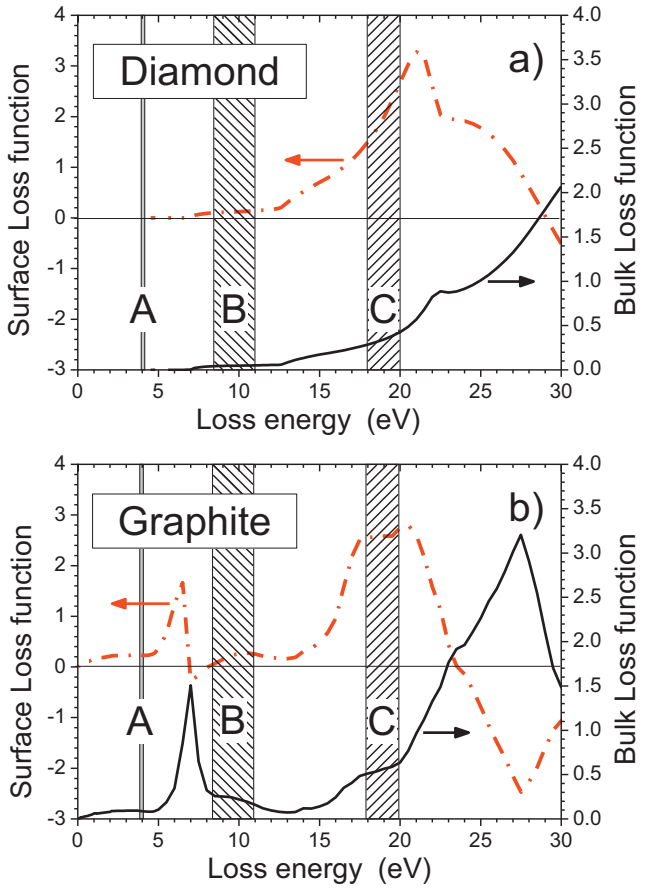

Fig. 7. Energy loss probabilities corresponding to the surface $S(\hbar\omega)$ (dashed lines) and bulk $B(\hbar\omega)$ (full lines) plasmon excitations, calculated using Eqs. (1a) and (1b) and tabulated optical index values: (a) diamond [25], (b) graphite (ordinary refractive index) [26]. Experimental peaks in the difference spectrum (Fig. 5) are depicted by the shaded areas; peaks B and C coincide with surface plasmon excitation due to some sp^2 phase.

[18,27,42]; however, Fig. 7 shows that this feature alone cannot be taken as a signature of the surface plasmon because the calculated surface plasmon peak of diamond (at 21.2 eV) overlaps the shoulder at 22.5 eV in the bulk plasmon (Fig. 7a).

Fig. 7a also shows that the calculated surface plasmon of diamond (21.2 eV) matches the shoulder observed at 21 eV in experimental spectra for as-grown and annealed diamond films; in contrast it is located at a larger loss energy value as compared with peak C (19 eV) in the difference spectrum of Fig. 5. Hence, we believe that peak C in the difference spectrum is not the signature of a surface plasmon of diamond.

In contrast, the experimental loss features near 10 ± 1 eV and 19 ± 1 eV are well described by the surface plasmon of graphite (Fig. 7b). Although peak B is rather weak, considered together peak B and C are consistent with the calculated surface plasmon using the graphite dielectric function; interestingly, Fig. 7b shows that the surface plasmon contribution at the location of peak B must be smaller than that at peak C position.

Since the matching of PEELS data with the surface plasmon of graphite apparently contradicts the absence of a "conductive surface" made of nanometer-size graphitized layer, alternative explanations could be interesting. On the one hand, some increase in the σ–σ^* inter band transition strength, expected near 12–13 eV [43], seems too high in energy to account for peak B. On the other hand, some loss features near 11 eV and 19 eV were observed in the electron energy loss distribution of a graphene single layer grown on copper, after desorption of some surface contamination

by thermal annealing at 300 °C, which is believed to remove defects and metastable sp^3 sites [44]. These features were respectively attributed to $\pi \rightarrow \sigma^*$ and $\sigma \rightarrow \pi^*$ single electron transitions, which may reveal distorted environments of carbon atoms.

Further work with single crystal rather than microcrystalline diamond may be helpful to address the PEELS signature and to investigate loss distribution broadening and surface plasmon enhancement effects.

5. Conclusion

The sensitivity of Photoelectron Energy Loss Spectroscopy has been investigated using the well-controlled surface reconstruction of microcrystalline diamond thin films upon UHV annealing at 1150 °C. This comparative study shows that PEELS detects surface effects which are not seen by UV Raman spectroscopy. After annealing, the bulk $(\sigma + \pi)$ plasmon of diamond at 34.5 eV is weakly attenuated but no evidence for surface graphitization is observed near 6 eV. Characteristic features at 10 ± 1 eV and 19 ± 1 eV in the energy loss distribution match the calculated optical surface plasmons in graphite-like materials; alternatively they also coincide with experimental plasmon losses in some graphene layers. This work shows that PEELS acquisition with standard XPS equipment gives a sensitive signature of weak effects in the diamond surface reconstruction, even in the absence of graphitization. It confirms that PEELS is a sensitive tool for surface dielectric function analysis, complementary to XPS chemical analysis.

Acknowledgment

One of us (C.G.) is grateful to the CNPq agency (Brazil) for a visiting researcher grant in the *Ciência Sem Fronteiras* programme.

References

[1] Auger and X-ray Photoelectron Spectroscopy, in: D. Briggs, M.P. Seah (Eds.), Practical Surface Analysis, vol. 1, second ed., John Wiley and Sons, Chichester, UK, 1990.
[2] S. Tougaard, Physical Review B 34 (1986) 6779.
[3] S. Tougaard, Surface and Interface Analysis 11 (1988) 453–472.
[4] A. Cohen Simonsen, F. Yubero, S. Tougaard, Physical Review B 56 (1997) 1612.
[5] W.S.M. Werner, Surface and Interface Analysis 31 (2001) 141–176.
[6] R.F. Egerton, Electron Energy-Loss Spectroscopy in the Electron Microscope, Second Edition, Plenum Press, New York, 1996.
[7] J.B. Cui, J. Ristein, L. Ley, Physical Review Letters 81 (1998) 429.
[8] F. Maier, M. Riedel, B. Mantel, J. Ristein, L. Ley, Physical Review Letters 85 (2000) 3472.
[9] J. Ristein, F. Maier, M. Riedel, M. Stammer, L. Ley, Diamond and Related Materials 10 (2001) 416.
[10] L. Diederich, O.M. Küttel, P. Aebi, L. Schlapbach, Surface Science 418 (1998) 219.
[11] P.K. Bachmann, W. Eberhardt, B. Kessler, H. Lade, K. Radermacher, D.U. Wiecher, H. Wilson, Diamond and Related Materials 5 (1996) 1378.
[12] C.H. Goeting, F. Marken, A. Gutierrez-Sosa, R.G. Compton, J.S. Foord, Diamond and Related Materials 9 (2000) 390.
[13] J.I.B. Wilson, J.S. Walton, G. Beamson, Journal of Electron Spectroscopy and Related Phenomena 121 (2001) 183.
[14] D. Ballutaud, N. Simon, H. Girard, E. Rezpka, B. Bouchet-Fabre, Diamond and Related Materials 15 (2006) 716.
[15] Sh. Michaelson, A. Hoffman, Diamond and Related Materials 15 (2006) 486–497.
[16] B.R. Stoner, G.H.M. Ma, S.D. Wolter, J.T. Glass, Physical Review B 45 (1992) 11067.
[17] S. Haq, D.L. Tunnicliffe, S. Sails, J.A. Savage, Applied Physics Letters 68 (1996) 469.
[18] M.S. Haque, H.A. Naseem, J.L. Shultz, W.D. Brown, S. Lal, S. Gangopadhyay, Journal of Applied Physics 83 (1998) 4421.
[19] J.C. Arnault, S. Saada, M. Nesladek, O.A. Williams, K. Haenen, P. Bergonzo, E. Osawa, Diamond and Related Materials 17 (2008) 1143.
[20] R. Klauser, J.M. Cheng, T.J. Chuang, L.M. Chen, M.C. Shih, J.C. Lin, Surface Science 356 (1996) L410–L416.
[21] F. Maier, R. Graupner, M. Hollering, L. Hammer, J. Ristein, L. Ley, Surface Science 443 (1999) 177–180.
[22] T. Frauenheim, U. Stephan, P. Blaudeck, D. Porezag, H.G. Busmann, W. Zimmermannedling, S. Lauer, Physical Review B 48 (1993) 18189–18202.
[23] G. Kern, J. Hafner, J. Furthmuller, G. Kresse, Surface Science 352–354 (1996) 745.
[24] T. Petit, J.C. Arnault, H.A. Girard, M. Sennour, P. Bergonzo, Physical Review B 84 (2011) 233407.
[25] D.F. Edwards, H.R. Philipps, in: E.D. Palik (Ed.), Handbook of Optical Constants of Solids, Academic, San Diego, 1985, p. 665.
[26] A. Borghesi, G. Guizzetti, in: E.D. Palik (Ed.), Handbook of Optical Constants of Solids, vol. 2, Academic, New York, 1991, pp. 449.
[27] S. Waidmann, M. Knupfer, B. Arnold, J. Fink, A. Fleszar, W. Hanke, Physical Review B 61 (2000) 10149.
[28] D. David, C. Godet, H. Sabbah, S. Ababou-Girard, F. Solal, V. Chu, J.P. Conde, Journal of Non-Crystalline Solids 358 (2012) 2019–2022.
[29] D. David, C. Godet, unpublished.
[30] K.M. McNamara, K.K. Gleason, D.J. Vestyk, J.E. Butler, Diamond and Related Materials 1 (1992) 1145.
[31] A.B. Fadjie, S. Ababou-Girard, C. Godet, Journal of Applied Physics 112 (2012) 113701.
[32] S. Waidmann, M. Knupfer, J. Fink, B. Kleinsorge, J. Robertson, Diamond and Related Materials 9 (2000) 722–727.
[33] M.L. Theye, V. Paret, Carbon 40 (2002) 1153.
[34] R. Haerle, E. Riedo, A. Pasquarello, A. Baldereschi, Physical Review B 65 (2001) 045101.
[35] N. Pauly, M. Novak, S. Tougaard, Surface and Interface Analysis (2013), http://dx.doi.org/10.1002/sia.5167.
[36] A.C. Ferrari, A. Libassi, B.K. Tanner, V. Stolojan, J. Yuan, L.M. Brown, S.E. Rodil, B. Kleinsorge, J. Robertson, Physical Review B 62 (2000) 11089.
[37] P. Reinke, M.G. Garnier, P. Oelhafen, Journal of Electron Spectroscopy and Related Phenomena 136 (2004) 239.
[38] A. Zebda, H. Sabbah, S. Ababou-Girard, F. Solal, C. Godet, Applied Surface Science 254 (2008) 4980–4991.
[39] C. Godet, D. David, H. Sabbah, S. Ababou-Girard, F. Solal, Applied Surface Science 255 (2009) 6598.
[40] N. Simon, H. Girard, D. Ballutaud, S. Ghodbane, A. Deneuville, M. Herlem, A. Etcheberry, Diamond and Related Materials 14 (2005) 1179.
[41] S.V. Pepper, Surface Science 123 (1982) 47.
[42] Y. Wang, H. Chen, R.W. Hoffman, J.C. Angus, Journal of Materials Research 5 (1990) 2378.
[43] L. Calliari, S. Fanchenko, M. Filippi, Carbon 45 (2007) 1410–1418.
[44] A. Siokou, F. Ravani, S. Karakalos, O. Frank, M. Kalbac, C. Galiotis, Applied Surface Science 257 (2011) 9785.